Earth Reinforcement, Ochiai, Yasufuku & Omine (eds) © 1996 Balkema, Rotterdam. ISBN 90 5410 833 9

Full scale laboratory testing on geosynthetics reinforced paved roads

Andrea Cancelli
University of Milan, Italy

Filippo Montanelli & Pietro Rimoldi
Tenax SpA, Italy

Aigen Zhao
Tenax Corporation, USA

ABSTRACT: The resistance to traffic loads of geosynthetics reinforced paved roads over soft soil has been investigated by means of extensive full scale laboratory testing, consisting of measuring the settlements distribution in a reinforced section when stressed cyclically with a load simulating a truck wheel. The rut depths were measured as a function of the number of cycles, of the aggregate thickness, of the subgrade shear strength and of the reinforcement type. The ability of the reinforcement to distribute the load over a wider subgrade surface area was monitored and analysed. The results of the reinforced sections have been compared with the corresponding unreinforced sections showing the advantages of the use of geosynthetics in increasing the road service life and savings in aggregate thickness.

1 INTRODUCTION

It has been well established that the inclusion of a geosynthetic reinforcement layer within a paved road section can substantially improve the overall strength and life of the road itself. Laboratory models of the reinforcing behaviour of the geosynthetics have been developed by several authors; however, most of them were limited in number of tests or performed in small boxes or on pavement sections with low structural number, thus they cannot be considered as full scale tests. The aim of this work was to perform laboratory tests as close as possible to reality (Haas, 1986) and (Beretta et. al., 1994).

2 TEST ARRANGEMENT

The road section has been reproduced using a very large metal box which has been filled in the lower half with loose sandy soil. Above it, a reinforcement layer was placed and then the remaining upper part of the box was filled with well graded and compacted crushed stone aggregate and finally with an asphalt layer. The dimensions of this box were 1.8 m x 0.9 m x 0.9 m. The box was vertically divided into halves by a removable metal plate.

Typically, a geosynthetic layer was placed only in one half of the box section, while the other half was left unreinforced to be used for comparison purposes. This technique allows a greater precision in determining absolute and relative reinforcement effects since all the properties of the soils in the two halves were exactly the same because the two parts of the box were filled at the same time using the same soil handling procedures. When testing the geosynthetics, the reinforcement layer was placed flat above the layer of loose soil and then folded at 90° at the box sides as shown in figure 1.

The reinforcement was folded to the metal box sides to model the anchorage of a geosynthetic in a typical wide road base: in this way failures of the road model during the test, due to the still relatively small dimensions of the box were prevented.

Up to 300,000 sinusoidal loading cycles have been applied through a circular loading plate having 300 mm diameter. The tests have been performed at a frequency of either 5 or 10 Hz and the load was ranging from 0 to 40 kN with an equivalent maximum applied pressure of 570 kPa. The vertical settlements (ruts) have been recorded as function of number of cycles together with the permanent deformation in the road section. The applied load, contact pressure and the loading plate dimension were selected as typical conditions for truck tire pressure and contact area. In fact, typically 40 kN is the semi-axle load, 570 kPa is the typical inflating tire pressure and 300 mm diameter can be assumed as the deformed tire contact area.

The sinusoidal cycle loading has been applied through a servohydraulic actuator controlled by an Instron 8580 digital multi-axis closed-loop controller and the rut depths were measured by a transducer inside the piston.

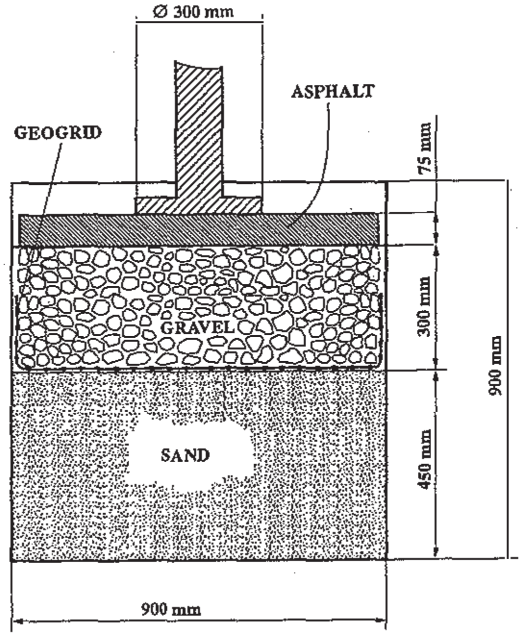

Figure 1 - Typical cross section of the testing apparatus showing the inner dimensions, the loading piston and the geogrid location.

The settlements and the elastic rebounds of the asphalt layers have been measured during the tests, under the loading plate, every 100 cycles.

The distribution of the permanent deformation on the aggregate was recorded during the tests by measuring the displacements of the asphalt surface in several locations, and of the asphalt/aggregate and aggregate/subgrade interfaces at the end of each test.

3 TYPES OF SOIL AND ASPHALT

Crushed limestone produced from oversize quarried aggregate with trace of sand aggregate was selected for the road base. This material is typically used for flexible road bases and for the construction of foundations. This material was partially washed in the quarry to remove the fine particles. The crushed stone gradation is shown in figure 2 as per ASTM D136. The maximum particle size of the aggregate was 30 mm. Hence, being the box size equal to 900 mm, the scale ratio with the aggregate was equal to 30: this high value ensures that no scale effect can influence the results.

The soft and compressible subgrade was simulated by means of about 450 mm of loose uniform sand having a uniformity coefficient U≈2, dry density γ_d=19.00 kN/m^3 and an optimum moisture content w = 15%. The sand grain

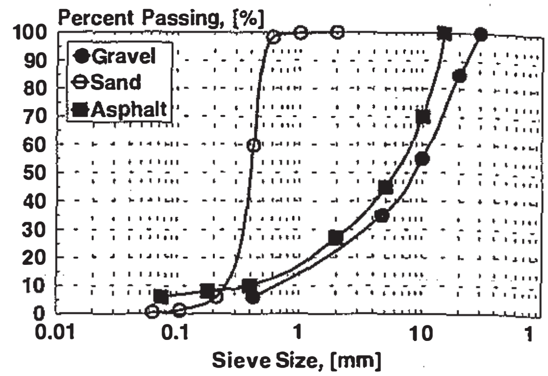

Figure 2 - Crushed limestone, sand and asphalt gradation curves

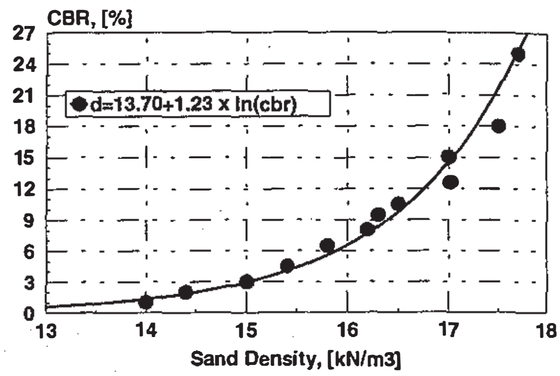

Figure 3 - CBR of Ticino sand versus density at 10% moisture content.

distribution is shown in figure 2 as per ASTM D136. This sand is called Ticino siliceous sand since it is dredged from the Ticino river.

A constant moisture content of 10% for the sand was selected for all the tests and an empirical relationship between the CBR and the soil dry density was determined using the test procedure outlined in ASTM D 1883 test method (see figure 3).

Several subgrade shear strengths have been used during the test trials, with CBR ranging from 1% up to 18%.

The different CBR values have been reproduced by means of 450 mm of Ticino sand placed at a moisture content of 10% and at a density following the regression curve in figure 3.

The CBR values have been preliminarly determined by means of laboratory tests using the standard CBR mould specimens as per ASTM D 1883 and in the test boxes prior to aggregate filling using a field CBR testing apparatus.

The gravel aggregate was placed in 300 mn thickness and compacted to achieve a density o about 17.50 kN/m^3. This relatively low density o the aggregate material was selected because it ha been found very difficult to get a higher density without overstressing the subgrade, with consequent pre-rutting.

The thickness of the asphalt layers has been kept constant and equal to 75 mm. The asphalt gradation curve is given in figure 2. The asphalt specifications were in accordance to the Italian highway department requirements.

4 TYPES OF GEOSYNTHETICS

The following geosynthetics have been tested:

A. multi-layer biaxially oriented polypropylene geogrids manufactured by continuous extrusion and orientation processing;

B. biaxially oriented polypropylene geogrids manufactured by punching and drawing a sheet;

C,D. biaxially oriented polypropylene geogrids manufactured by continuous extrusion and orientation processing;

E. polyester woven geogrid;

F. slit film woven polypropylene geotextile.

The characteristics of the tested geosynthetics are highlighted in table 1.

The performances of the geosynthetic layers have been investigated by placing them at the subgrade-aggregate interface or in some cases by placing an additional layer at mid thickness of the aggregate layer (test n. 6).

5 TEST RESULTS AND DESIGN CHARTS

The testing program is highlighted in Table 2. As it can be noticed, 4 CBR values have been reproduced in the tests, namely CBR equal to 1,3,8,18.

The CBR/products combinations have been decided in order to allow a sound comparison between different geosynthetics in the same soil conditions and between the behaviour of the same geosynthetic with different soil bearing capacities.

The tests results have been analysed and plotted to show the following results:

1. comparisons between reinforced and unreinforced sections, see figure 4;
2. comparisons between reinforced sections at different CBRs, see figure 4;
3. comparisons between reinforced and unreinforced sections with different aggregate thickness, see figure 5;
4. comparison between geosynthetics, fig. 6 and 7.

Ruts geometry for reinforced and unreinforced sections have been analysed to determine differences in depth and shape of the deformed sections, order to evaluate the reinforcement function played by the different geosynthetics.

Table 1. Geosynthetic type and properties

Geosynthetic type	Tensile strength (MD x TD), kN/m	Mean mesh dimensions, mm
A - TENAX MS220	15.0 x 20.5	20 x 25 Random
B - TENSAR BX1100	12.5 x 20.5	25 x 50 Rectangular
C - TENAX MS1000	14.0 x 19.7	30 x 40 Rectangular
D - TENAX LBO 301 SAMP	19.5 x 31.6	30 x 40 Rectangular
E - FORTRAC 35/20-20	55 x 20	20 x 20 Rectangular
F - AMOCO 6070	48 x 40	---

Table 2. Summary of the testing program (N.R.=not reinforced).

Test n.	Geogrid type	Soil CBR %	Soil density kN/m^3	Testing Frequency Hz
3	N.R.	1	13.0	5
4	A	1	13.0	5
5	B	1	13.0	5
6	2 X A	1	13.0	5
7	C	1	13.0	5
8	D	1	13.0	5
9	N.R.	3	15.0	10
10	A	3	15.0	10
11	D	3	15.0	10
15	E	3	15.0	10
16	F	3	15.0	10
25	N.R.	8	16.2	10
26	A	8	16.2	10
1	N.R.	18	17.5	10
2	A	18	17.5	10

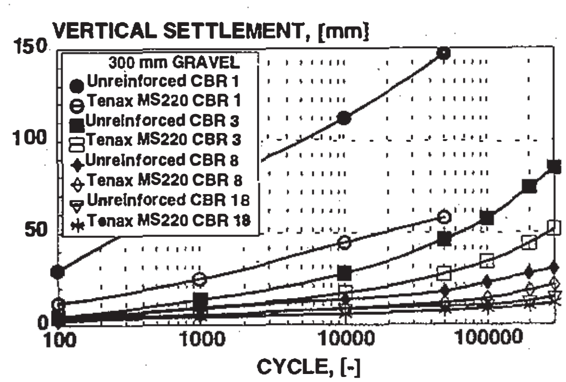

Figure 4 - Comparisons between reinforced and unreinforced sections at several CBRs and with 300 mm aggregate thickness.

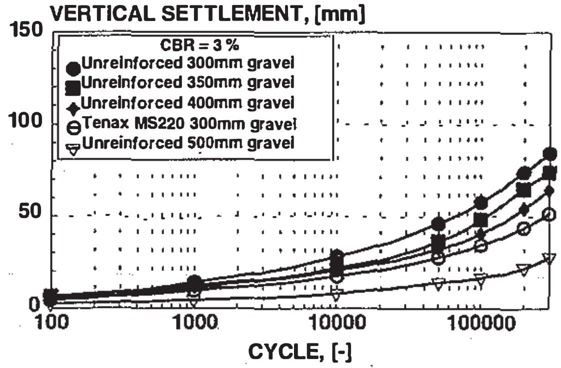

Figure 5 - Comparisons between reinforced and unreinforced sections at CBR = 3.0% for several aggregate thicknesses.

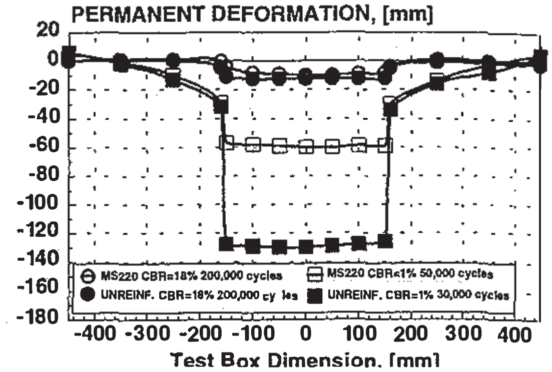

Figure 8 - Typical ruts geometry for unreinforced and reinforced sections for different CBRs.

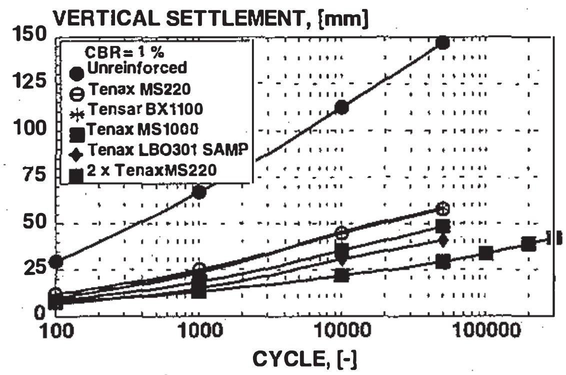

Figure 6 - Comparison between geosynthetics at CBR = 1.0 %.

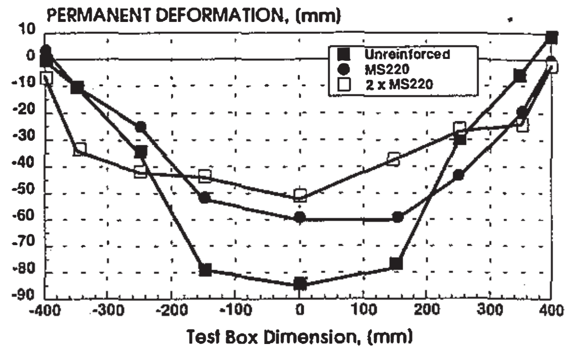

Figure 9 - Typical deformed shape of the asphalt-aggregate interface at the end of a test.

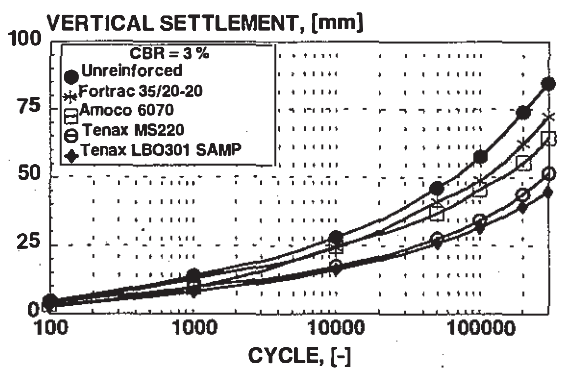

Figure 7 - Comparison between geosynthetics at CBR = 3.0 %.

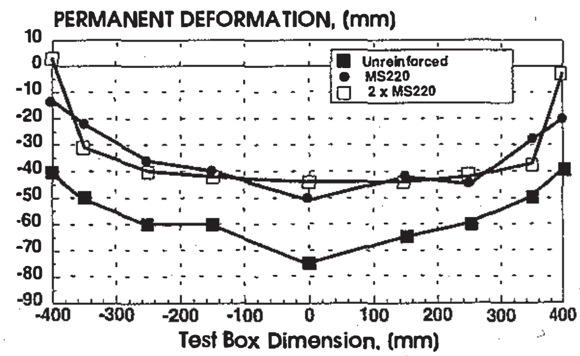

Figure 10 - Typical deformed shape of the aggregate-subgrade interface at the end of a test.

Typical ruts geometry for CBR=1 and 18 are shown in figure 8.

The deformed shape of the asphalt - aggregate and aggregate-subgrade interfaces, at the end of a test, are shown in figure 9 and figure 10. As it can be noticed by analysing figure 8, the deformation curves are very sharp in proximity of the loading plate area. In fact, the failure type for all the performed tests has been a puncture failure by shearing the asphalt layer not sufficiently supported by the layer underneath. This type of failure is essentially due to the type of subgrade used during the tests. In fact the soft sand has a very high compressive behaviour and largely reduces its volume when compressed. Moreover the rigid loading plate generated high shear stresses on the asphalt at its edges.

Anyway figure 9 and 10 clearly shows that, for reinforced sections, the load was evenly distributed by the asphalt and the reinforcement on the

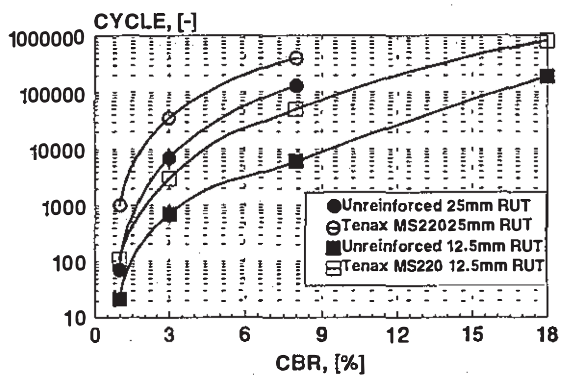

Figure 11 - CBR vs. cycle number for reinforced and unreinforced sections at given rut depth.

aggregate and subgrade layers, which haven't suffered any punching failure. It is interesting to note that the maximum settlement, both at the asphalt-aggregate and at the aggregate - subgrade interfaces, is much lower for the geogrid reinforced sections than for the unreinforced ones.

Figures 9 and 10 also show that 2 layers of geogrids, one at the base and one at mid thickness of the aggregate layer, are able to provide more stiffening to the base layer than 1 geogrid only: in fact with 2 geogrids, the deformation is much more uniform and the maximum settlement is lower.

Suggested design charts (function of the subbase soil shear strength, number of cycles, allowed rut depth and layer coefficient ratio) are presented in figure 11, 12 and 13 to allow engineers to design successful reinforced paved roads.

In figure 11, the relationship between unreinforced and geogrid reinforced road sections, based upon actual rut depth, is shown.

Figure 12 shows the traffic improvement factor (the ratio of the number of load cycles for the reinforced section to that of unreinforced section at a given rut depth) for the Tenax MS220 geogrid. Figure 12 is simply obtained from the ratios of the related points in figure 11.

The chart in figure 12 allows to evaluate the increase of design life (in terms of increased number of vehicles passing) which can be achieved by simply placing a geogrid in a given road section. The AASHTO (Americal Association of State Highway and Transportation Officials) design method for flexible pavement, which is a regression method based on the results of road tests, is widely used for road design. In the AASHTO method the structural contribution of geosynthetics on flexible pavements can be quantified by the increase in the structural layer coefficient of the aggregate base course. The AASHTO method utilises an index named structural number (SN) to indicate the necessary combined structural capacity of all pavement layers overlying the subgrade. SN is a function of subgrade strength, expected traffic intensities, pavement life, and climatic conditions.

A simple design equation is used in AASHTO method:

$$SN = a_1 \cdot t_1 + a_2 \cdot t_2 + a_3 \cdot t_3 \qquad (1)$$

where the subscript 1, 2 and 3 refer to the asphalt wearing course, aggregate base course and subbase course (if applicable), and a_1, a_2, a_3 are layer coefficients used to characterise the structural capacity of different layers in the pavement system; t_1, t_2 and t_3 are their thickness.

The layer coefficients can be found from AASHTO design table. The better the course material, the higher the layer coefficient. The structural number is directly proportional to the layer coefficients and thicknesses.

The structural contribution of a geosynthetic in a flexible pavement system can be quantified by the increase in the layer coefficient of the aggregate base course. Equation (1) now becomes:

$$SN = a_1 \cdot t_1 + a_2 \cdot (\alpha_r / \alpha_u) \cdot t_2 \qquad (2)$$

where α_r/α_u is the layer coefficient ratio.

Therefore the structural contribution of geosynthetic can be determined through the layer coefficient ratio, which is defined as:

$$\alpha_r / \alpha_u = (SN_r \cdot t_r) / (SN_u \cdot t_u) \qquad (3)$$

where α_r/α_u is the layer coefficient ratio, SN_r and SN_u are the structural numbers for reinforced and unreinforced pavement section, and t_r and t_u are the base course thicknesses for reinforced and unreinforced section respectively.

As a result, a reduction in aggregate thickness can be achieved by the use of an appropriate geosynthetic:

$$t_2 = \frac{SN - a_1 \cdot t_1}{(\alpha_r / \alpha_u) \cdot a_2} \qquad (4)$$

or instead, the asphalt thickness can be reduced:

$$t_1 = \frac{SN - (\alpha_r / \alpha_u) \cdot a_2 \cdot t_2}{a_1} \qquad (5)$$

Figure 13 shows the layer coefficient ratio, for Tenax MS220. This chart has been obtained by determining the values of SN_r and SN_u on the base of a Design Serviceability Index equal to 2 and a Regional Factor equal to 1, as defined in the AASHTO design method.

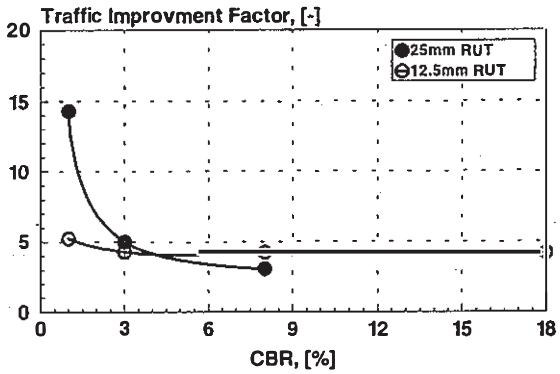

Figure 12 - Traffic improvement factor Vs. CBR for two rut depth for Tenax MS220 geogrids.

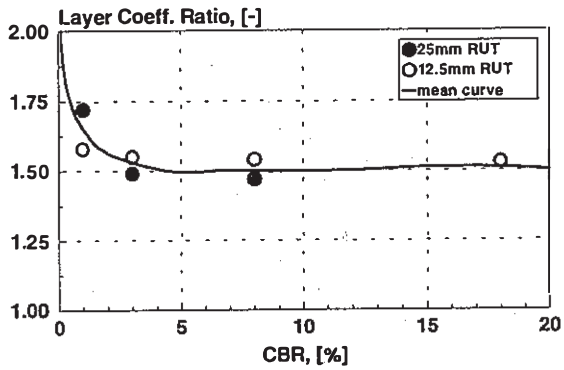

Figure 13 - Layer coefficient ratio vs. Subgrade CBR value for Tenax MS220 geogrids..

6 CONCLUSIONS

The results obtained from this experimental research work support the following conclusions:

1. A geogrid placed at the subbase/aggregate interface is effective and probably ideal for increasing the service life of a paved road. For limiting the rut depth at very low CBRs, two geogrid layers are suggested with one of them placed at mid thickness of the gravel section (figure 4);
2. The geogrid layers are able to mobilise stresses within the reinforced sections, preventing local shear failure and deformations (figure 8). Two layers of geogrids, compared to one layer only, provide a more uniform distribution of the load and decrease the maximum settlement both at the asphalt-aggregate and aggregate-subgrade interfaces (figures 9 and 10).
3. At a given maximum settlement, a geogrid reinforced gravel base is equivalent to a much thicker unreinforced base (figure 5).
4. The Tenax MS 220 multi-layer geogrid, even being relatively light in weight but having a mesh opening suitable for the dimensions of the aggregate and subgrade soil, provides the best results in reinforcing the road structure. The reinforcing capacity of the multi-layer geogrid can be mobilized at lower deformation than the typical heavier single layer geogrid.
5. No major differences have been found between the different single layer integral geogrids.
6. The percent reduction of rutting increase with reducing the subgrade CBR, for all the tested geosynthetics (figures 6 and 7).
7. The Traffic Improvement Factor for longer service life greatly increases for deep allowed ruts, lower CBR values and lower pavement structural number (figure 12).
8. The structural layer coefficient of the aggregate can be largely increased by a geogrid layer, having a layer coefficient ratio ranging from 2 to 1.5, depending mainly on the subgrade CBR (figure 13).
9. Design charts have been presented (figures 12 and 13). Due to the large dimensions of the reinforced sections and the number of tests performed, these charts are a valuable tool for the design of paved roads reinforced with geosynthetics.

ACKNOWLEDGEMENT

The Authors wish to thank Mr. Massimiliano Zinesi for his invaluable contribution during testing and Mrs. Stefania Brambilla for the preparation of this paper.

REFERENCES

American Association of State Highway and Transportation Officials, "AASHTO interim guide for design of pavement structures", Washington, (1996)

ASTM D-136 - 94, "Standard test method for sieve analysis of fine and coarse aggregates", *ASTM Volume 04.02*, Philadelphia, (1994)

ASTM D-1883 - 94. "Standard test method for the CBR (California Bearing Ratio) of laboratory-compacted soil", *ASTM Volume 04.08*, Philadelphia, (1994)

Beretta L., Cancelli A., Montanelli F., Rimoldi P. "Full scale laboratory tests on geosynthetic reinforced roads on soft soil", *5th International Symposium on Geosynthetics*, Singapore, (1994)

Haas, R., "Granular base reinforcement of flexible pavements using Tensar geogrids", *Tensar internal test report TTN:BR1*, (1986).